

# CMOS Capacitive Biosensors for Highly Sensitive Biosensing Applications

An-Yu Chang and Michael S.-C. Lu

**Abstract**—Magnetic microbeads are widely used in biotechnology and biomedical research for manipulation and detection of cells and biomolecules. Most lab-on-chip systems capable of performing manipulation and detection require external instruments to perform one of the functions, leading to increased size and cost. This work aims at developing an integrated platform to perform these two functions by implementing electromagnetic microcoils and capacitive biosensors on a CMOS (complementary metal oxide semiconductor) chip. Compared to most magnetic-type sensors, our detection method requires no externally applied magnetic fields and the associated fabrication is less complicated. In our experiment, microbeads coated with streptavidin were driven to the sensors located in the center of microcoils with functionalized anti-streptavidin antibody. Detection of a single microbead was successfully demonstrated using a capacitance-to-frequency readout. The average capacitance changes for the experimental and control groups were  $-5.3$  fF and  $-0.2$  fF, respectively.

## I. INTRODUCTION

With the advances in micro-system technologies, lab-on-chips have become a major research area for miniaturizing biological assays towards point-of-care diagnostics. An ideal lab-on-chip is desired to be capable of manipulating and sensing biological samples. With these dual functions, various samples can be sorted and detected with a shortened response time and sensitivity can be enhanced by pre-concentration of diluted samples. In many applications, microparticles functionalized with target biomolecules are used for convenient manipulation and detection; for example, magnetic microbeads have been utilized extensively in biomolecule separation and purification, immunoassays, magnetic resonance imaging, and hyperthermia. They can be conveniently manipulated by using permanent magnets or electromagnets. As compared to fluorescent labeling for biosensing, magnetic microbeads are relatively stable over time because the magnetism is not affected by reagent chemistry or subject to photo-bleaching.

A magnetic label can be detected by SQUID (superconducting quantum interference device) [1], magnetoresistive sensors [2], nuclear magnetic resonance [3], Hall sensors [4], inductive coils [5], and optical sensors [6]. Manipulation and detection of magnetic microparticles have been demonstrated by many lab-on-chips [7]. Most of them rely on external means to perform one of the functions, leading to increased size, complexity, and cost of the overall system. A miniaturized system can be implemented by on-chip

integration of these capabilities. Several works [2] reported integrated chips consisting of current-carrying wires to manipulate and magnetize microbeads and magnetoresistive sensors for microbead detection. For implementation of a large array, it is often desirable to use an integrated-circuit process to facilitate signal routing, multiplexing, and processing.

Compared to most of the aforementioned magnetic sensing techniques, capacitive sensing does not require additional deposition of magnetic thin films and application of magnetic fields for detection. A capacitance change due to a dielectric property change and/or carried electric charges is induced when a magnetic microbead binds to electrically biased electrodes. Most of the capacitive biosensors are not implemented in an integrated-circuit process (e.g. CMOS). Capacitive biosensors fabricated in a CMOS process [8] can provide enhanced signal-to-noise ratio by minimizing the effect of parasitic capacitances observed at the sensing node. To date, capacitive detection of a single magnetic microbead has not been demonstrated by a CMOS biochip. Toward this end, this work presents a CMOS capacitive sensor array with integrated microcoils for magnetic manipulation. The active manipulation capability effectively enhances the probability of capturing a single magnetic microbead for the ensuing detection. Each microcoil can attract a microbead to its center where a capacitive sensor is located. The capacitance change leads to an output frequency change of the oscillator-based sensing circuit. Detection of a single microbead functionalized with streptavidin is successfully demonstrated. More details regarding to the design and measurement of the CMOS chip are presented in the following sections.

## II. METHOD

### A. Operating Principle

A two-polysilicon-four-metal (2P4M)  $0.35\text{-}\mu\text{m}$  CMOS process is utilized for fabrication of the  $8\times 8$  micro-manipulation and sensor array. As shown by the cross-sectional view in Fig. 1(a), each basic element in the array consists of a microcoil for electromagnetic actuation and a set of interdigitated microelectrodes in its center for capacitive detection. The microcoil is constructed using multiple metal layers provided by the CMOS process in order to increase the number of turns and thus the produced electromagnetic force. The passivation thin films for chip protection are kept on top of microcoils but removed in the electrode areas by foundry's dry etching process. The thin intermetal silicon dioxide ( $\sim 0.3\ \mu\text{m}$ ) remaining on electrode surface is used for immobilizing bio-recognition elements, such as anti-streptavidin antibody used in this work. As shown

\*Research supported by National Science Council, Taiwan, R.O.C.

An-Yu Chang and Michael S.-C. Lu are with the Institute of Electronics Engineering, National Tsing Hua University, Taiwan, R. O. C. (e-mail: sclu@ee.nthu.edu.tw).

in Fig. 1(b), magnetic microbeads functionalized with streptavidin are electromagnetically moved toward the sensor in the microcoil center. The electrode is slightly larger than a microbead, thereby allowing only one microbead to remain on its surface for specific binding and the following capacitive detection [Fig. 1(c)]. The magnetic microbead used in this study is a polymer (polystyrene) microspheres containing a large number of nanomagnets made of iron oxide. The capacitance change near the bead-electrode interface is attributed to a dielectric property change and/or electric charges.

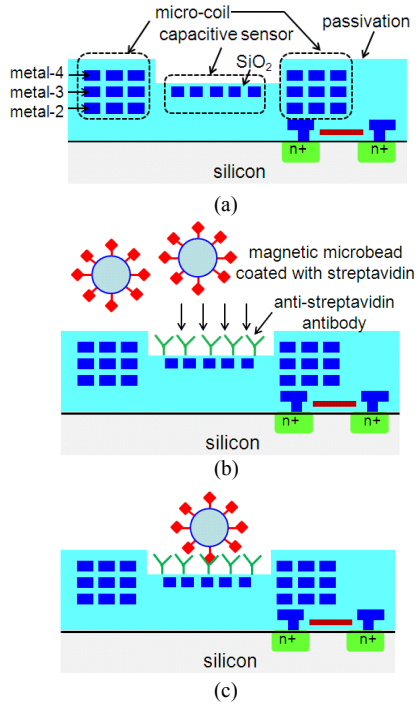


Figure 1. Operating principle of magnetic microbead-based manipulation and capacitive detection: (a) Cross-sectional view of the fabricated CMOS chip. (b) Magnetic actuation of streptavidin-coated magnetic microbeads toward the capacitive sensor with functionalized anti-streptavidin antibody. (c) Capacitive detection of the remaining microbead after specific binding.

### B. Surface Functionalization and Immobilization

CMOS chips were firstly washed by ethanol and acetone solutions for 10 min respectively to remove contaminants and introduce  $-OH$  on the oxide surface. Then the chips were immersed in 2% APTES ethanol solution to introduce amino groups on the oxide surface. The chips were then washed with ethanol to remove unbound APTES. In the following step, the chips were immersed in 2.5% glutaraldehyde solution prepared from 10 mM PBS (pH = 7.0) for 2 h followed by PBS wash. Finally, 10  $\mu M$  anti-streptavidin antibodies were coupled to the sensor surface in PBS for 10 h. The un-reacted aldehyde groups were blocked by mixing with 50-mM ethanolamine for 1 h followed by PBS wash.

### C. Microcoil and Capacitive Biosensor Array

Implementation of a large and scalable manipulation and biosensor array in a CMOS process is facilitated by the

on-chip electronics for signal processing and multiplexing. As shown by the schematic in Fig. 2(a), the chip design comprises  $8 \times 8$  microcoils and the center of each microcoil contains a capacitive sensor. Two microcoil designs are implemented, one (type A) with a narrower linewidth (1  $\mu m$ ) but more turns and the other (type B) with a wider linewidth (10  $\mu m$ ) and less turns. Multiple CMOS metallization layers are used to form 25 turns and 20 turns for the type-A and type-B microcoils whose resistances are 350 and 40  $\Omega$ , respectively. There are four rows of type-A and type-B microcoils respectively on the chip. As illustrated in Fig. 2(a), electromagnetic driving of each microcoil is controlled by column/row decoders. The current flowing through each microcoil is provided by a current-mirror circuit whose current value is adjustable up to 30 mA through a three-bit decoder control. It is desired to produce a magnetic force in the order of tens of piconewtons for driving magnetic microbeads.

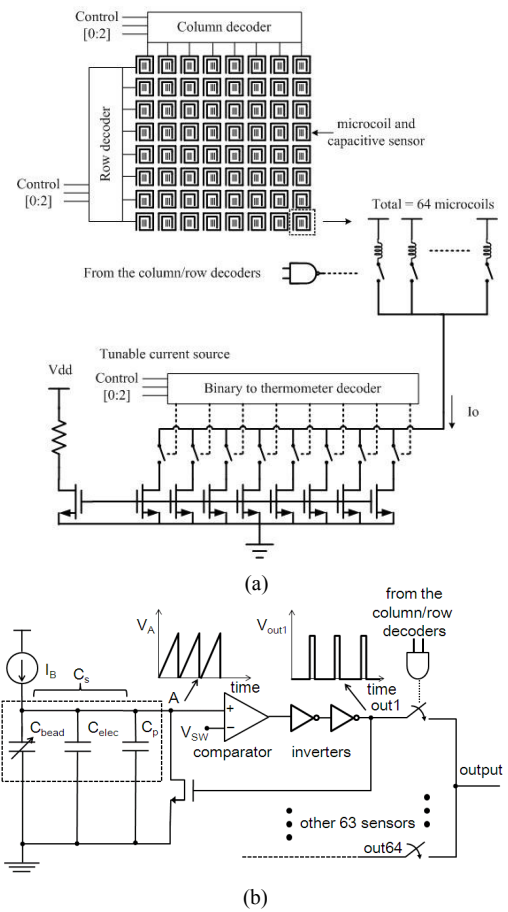


Figure 2. (a) Schematic of the CMOS micro-manipulation and biosensing array. (b) Schematic of the capacitive sensing circuit.

The interdigitated microelectrodes used for capacitive detection contain five pairs of 10- $\mu m$  long electrodes separated by a gap of 0.5  $\mu m$ . The electrode size is designed slightly larger than the magnetic microbead in order to demonstrate single-bead detection. Electric field lines across a smaller electrode gap are more effectively affected by an attached magnetic microbead to increase the capacitance change. The choice of 0.5  $\mu m$  is the minimum value allowed

by the foundry's design rules. Schematic of the CMOS oscillator readout is depicted in Fig. 2(b). The comparator in the circuit triggers the charging and discharging of the capacitor ( $C_s$ ) at a switching level  $V_{SW}$  and results in a pulse stream whose frequency varies with  $C_s$  as represented by:

$$f = \left[ \frac{C_s \cdot V_{SW}}{I_B} + \tau_d \right]^{-1} \quad (1)$$

where  $I_B$  is the bias current and  $\tau_d$  is the time delay caused by the comparator and the inverter delay stage. The output frequency is inversely proportional to the capacitance  $C_s$  with a negligible  $\tau_d$ . The capacitor  $C_s$  comprises the interdigitated microelectrode, represented by  $C_{elec}$ , in parallel with the parasitic and circuit input capacitances, represented by  $C_p$ , and the bead-electrode interface capacitance  $C_{bead}$ . Since the capacitances  $C_{elec}$  and  $C_p$  are positively charged by the current source, more positive or negative charges at the bead-electrode interface form an effective positive or negative capacitance that increases and decreases the total capacitance  $C_s$ . The value of  $C_{elec}$  is analyzed by finite-element simulation to be 7 fF. Compared to non-integrated capacitive sensors, capacitive sensitivity is significantly enhanced by monolithic integration to minimize the capacitance  $C_p$ . As depicted in Fig. 2(b), when the ramp signal  $V_A$  produced by the charged capacitor  $C_s$  reaches the switching level of the comparator, the reset transistor is turned on to discharge the capacitor to ground potential. Digital output pulses are automatically sustained by the feedback loop. Each output in the  $8 \times 8$  sensor array is sequentially measured by control of the column/row decoders.

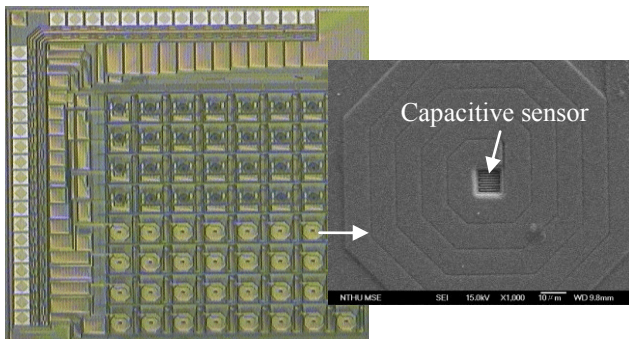


Figure 3. Micrograph of the CMOS chip and scanning electron micrograph of one of the type-B microcoils containing a capacitive sensor.

### III. EXPERIMENT

Fig. 3 shows the micrograph of the CMOS chip and the scanning electron micrograph of a type-B microcoil with a capacitive sensor in the center. Output waveforms were monitored on a digital oscilloscope (Agilent DSOX 3014A) and pulse frequencies were recorded. Pulse frequencies of the  $4 \times 8$  sensors surrounded by the type-A microcoils were measured to be  $5.245 \pm 0.435$  MHz in air, and those of the ones surrounded the type-B microcoils were  $4.06 \pm 0.33$  MHz. The capacitances for the two cases were calculated to be  $23.3 \pm 1.9$

fF and  $30.1 \pm 2.4$  fF, respectively, for  $I_B = 200$  nA and  $V_{SW} = 1.65$  V. The difference is owing to that the routing wire with respect to the type-B microcoil produces a larger parasitic capacitance. Based on a simulated electrode capacitance  $C_{elec}$  of 7 fF, the capacitances  $C_p$  for the two cases are about 16 and 23 fF, respectively.

Sensor outputs were then measured during the surface modification and functionalization steps after adding APTES, glutaraldehyde, anti-streptavidin antibody, and ethanolamine. Each sensor was recorded for one second, so it took 64 seconds to complete one measurement of the  $8 \times 8$  array. The capacitance increase associated with APTES could be owing to that the amino group ( $pK_a > 9$ ) was protonated to  $-\text{NH}_3^+$  to result in more positive charges. The capacitance change associated with the electrically neutral glutaraldehyde varied within  $\pm 5\%$  of the nominal values. The capacitance increased by less than 10% after adding anti-streptavidin antibody, which could be attributed to a change of dielectric property and/or electric charges at the interface. The capacitance decrease due to ethanolamine could be due to the produced negative charges, since COOH and  $\text{NH}_3^+$  of anti-streptavidin antibody could be converted to  $\text{COO}^-$  and  $\text{NH}_2$  respectively due to an increased pH by adding 50 mM ethanolamine.

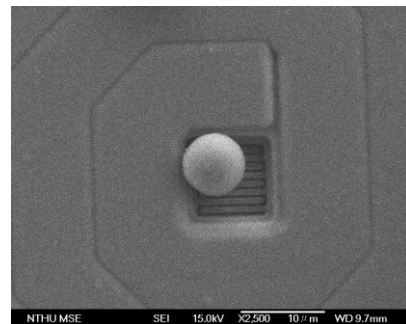


Figure 4. Scanning electron micrograph of a type-B microcoil with a captured microbead after specific binding.

In the next step, solution containing streptavidin-coated magnetic microbeads was diluted by 10 mM PBS and added to the chip by a micropipette. The microcoils were turned on in advance so the beads were driven before they landed on surface; otherwise more driving current was required to overcome surface adhesion force. To save power consumption, each row of microcoils was turned on sequentially for 1/8 second in a repeated manner. It was found that the type-A and type-B microcoils required about 10 mA and 25 mA respectively to move microbeads to their center. After specific binding of streptavidin and anti-streptavidin antibody on sensor surface, the chip was washed and dried in air. Fig 4 shows the scanning electron micrograph of a type-B microcoil with a captured microbead.

Fifteen sensors of the array showed a captured microbead. Fig. 5(a) shows the result of one of these sensors. The two curves in the figure represent the measurements where the chip was placed in air to dry after adding ethanolamine (i.e., before adding microbeads) and manipulation of microbeads, respectively. Both output frequencies gradually increased due to a decreased interface capacitance resulting from a gradually reduced dielectric constant while dried in air. The final

frequency for the sensor with a captured microbead was higher than the other curve, indicating a decrease in the overall capacitance  $C_s$ . For the sensors without a captured microbead (control group), the measured final frequencies of the two curves as shown in Fig. 5(b) were almost the same as expected.

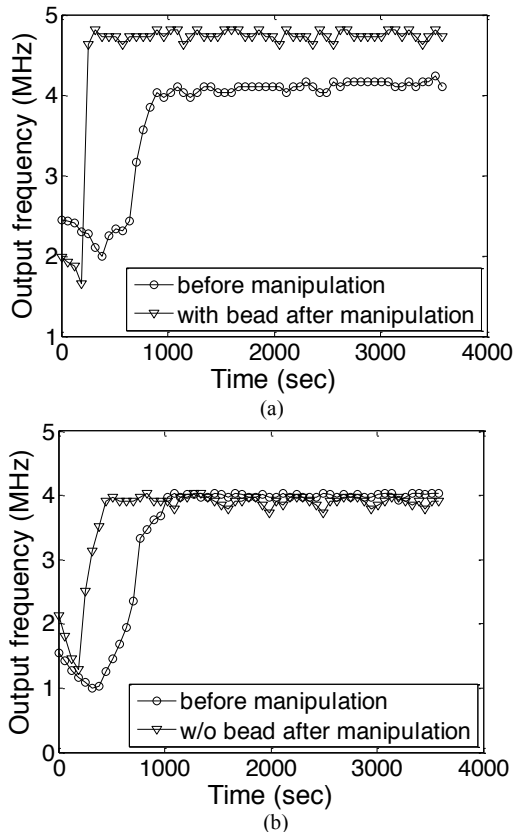


Figure 5. Measured output frequencies of capacitive sensors before and after magnetic manipulation: (a) one of the sensors with a captured microbead; (b) One of the sensors without a microbead.

The decreased bead-electrode interface capacitance due to a captured microbead could be attributed to the produced negative changes produced from two sources: (1) streptavidin coated on microbeads carries negative charges in the solution ( $\text{pH} \approx 7$ ) due to its isoelectric point ( $\sim 5$ ); (2) the charging and discharging waveform (0 to 1.65 V) on sensing electrodes produces a positive root-mean-square dc voltage that polarizes the microbead polymer to generate negative charges near the bead-electrode interface. The smallest and largest capacitance changes of the fifteen sensors with a captured microbead were  $-2.1$  fF and  $-10.2$  fF, respectively. The average capacitance change was  $-5.3$  fF with a standard deviation of  $2.5$  fF. The other sensors without a microbead showed much less capacitance changes ranging between  $-1.9$  fF to  $1.2$  fF, with an average of  $-0.2$  fF and a standard deviation of  $0.7$  fF. The measured result demonstrates that the average capacitance changes for the experimental and control groups differ by a ratio of more than an order of magnitude. It is reasonable to assume that the detectable capacitance change varies linearly with the microbead size. Therefore our sensor array should still be able to detect a microbead of  $1 \mu\text{m}$  in diameter.

#### IV. CONCLUSION

This work presents the first attempt to integrate microcoils and capacitive sensors to implement a monolithic micro-manipulation and biosensing array. Magnetic microbeads are moved to the desired sensor locations by on-chip magnetic actuation without requiring an external magnet. Single-microbead detection is successfully demonstrated by capacitive sensors with a similar size of a microbead. The associated capacitance change is quite small in the femto-farad range, which justifies the need for monolithic sensor integration to enhance capacitive sensitivity. The technology presented in this work is especially useful for building large DNA arrays and immunoassays to provide detection of multiple samples and large amount of data for statistical analysis. Without on-chip circuitry, the number of fabricated sensing devices is commonly limited by the difficulty to complete signal routing, whereas the issue of scalability does not exist for our work. In addition, as compared to other CMOS magnetic sensors, our capacitive sensors require no additional deposition of magnetic thin films and application of magnetic fields for detection.

#### ACKNOWLEDGMENT

The authors would like to thank the National Chip Implementation Center for chip fabrication and the National Center for High-Performance Computing for support of simulation software. We also thank Prof. Yuh-Shyong Yang and Dr. Chih-Heng Lin for their valuable suggestions.

#### REFERENCES

- [1] Y. R. Chemla, H. L. Grossman, Y. Poon, R. McDermott, R. Stevens, M. D. Alper and J. Clarke, "Ultrasensitive magnetic biosensor for homogeneous immunoassay," *Proc. Natl. Acad. Sci. USA*, vol. 97, pp. 14268-14272, 2000.
- [2] X. J. A. Janssen, L. J. van IJzendoorn and M. W. J. Prins, "On-chip manipulation and detection of magnetic particles for functional biosensors," *Biosens. Bioelectron.*, vol. 23, pp. 833-838, 2008.
- [3] N. Sun, Y. Liu, H. Lee, R. Weissleder and D. Ham, "CMOS RF biosensor utilizing nuclear magnetic resonance," *IEEE J. Solid-State Circuits*, vol. 44, pp. 1629-1643, 2009.
- [4] K. Togawa, H. Sanbonsugi, A. Lapicki, M. Abe, H. Handa and A. Sandhu, "High-sensitivity InSb thin-film micro-Hall sensor arrays for simultaneous multiple detection of magnetic beads for biomedical applications," *IEEE Trans. on Magnetics*, vol. 41, pp. 3661-3663, 2005.
- [5] H. Wang, Y. Chen, A. Hassibi, A. Scherer and A. Hajimiri, "A frequency-shift CMOS magnetic biosensor array with single-bead sensitivity and no external magnet," *IEEE Int. Solid-State Circuits Conference (ISSCC) Tech. Dig.*, pp. 438-439, 2009.
- [6] U. Lehmann, M. Sergio, S. Pietrocola, E. Dupont, C. Niclass, M. A. M. Gijs and E. Charbon, "Microparticle photometry in a CMOS microsystem combining magnetic actuation and in situ optical detection," *Sens. Actuators. B (Chem.)*, vol. 132, pp. 411-417, 2008.
- [7] K. Smistrup, B. G. Kjeldsen, J. L. Reimers, M. Dufva, J. Petersen and M. F. Hansen, "On-chip magnetic bead microarray using hydrodynamic focusing in a passive magnetic separator," *Lab Chip*, vol. 5, pp. 1315-1319, 2005.
- [8] E. Ghafar-Zadeh, M. Sawan and D. Therriault, "A  $0.18\text{-}\mu\text{m}$  CMOS capacitive sensor lab-on-chip," *Sens. Actuators A*, vol. 141, pp. 454-462, 2008.